Artificial Electro-Optical Neuron Integrating Hot Electrons in a Mott Insulator

Danylo Babich, Laurent Cario, Benoit Corraze, Maciej Lorenc, Julien Tranchant, Roman Bertoni, Marco Cammarata, Hervé Cailleau, Etienne Janod

Artificial electro-optical neuron integrating hot electrons in a Mott insulator

Danylo Babich,[1] Laurent Cario,[1,*] Benoit Corraze,[1] Maciej Lorenc,[2] Julien Tranchant,[1] Roman Bertoni,[2] Marco Cammarata,[2] Hervé Cailleau,[2] Etienne Janod,[1,*]

[1] *Institut des Matériaux Jean Rouxel (IMN), Université de Nantes, CNRS, 2 rue de la Houssinière, F-44322 Nantes, France*
[2] *Institut de physique de Rennes, Université de Rennes 1, Campus de Beaulieu 263 avenue du Général Leclerc, 35042 Rennes CEDEX, France*

** Laurent.Cario@cnrs-imn.fr,* Etienne.Janod@cnrs-imn.fr*

Abstract

Mott insulators are a class of strongly correlated materials with emergent properties important for modern electronics applications, such as artificial neural networks. Under electric field, these compounds undergo a resistive switching that may be used to build up artificial neurons. However, the mechanism of this resistive switching is still under debate and may depend on the Mott material involved. Some works suggest an electronic avalanche phenomenon, while others propose an electrothermal scenario. As electric pulses produce both Joule heating and hot carriers, disentangling their respective roles requires the use of another external stimulus. Here, an ultrashort light pulse is used to tune the number of photogenerated carriers and the energy provided to the system. In these pump-pump-probe experiments, a crystal of the Mott insulator $GaTa_4Se_8$ is simultaneously excited by electric and laser pulses while an electric probe monitors its conductivity. The study shows that the resistive switching is affected by the number of generated photocarriers rather than by the accumulation of energy deposited by the femtosecond laser. It supports therefore a mechanism driven by a hot carriers' generation. Finally, our work opens the possibility to build up an artificial electro-optical «Mott» neuron tuned by a femtosecond laser pulse.

PACS: 07.05.Mh,

1. INTRODUCTION

Modern Artificial Intelligence (AI) technology is currently based on the emulation of the biological neural networks on classical von Neumann computers. [1] However, the current approach is less efficient than the mammal brain in terms of energy consumption. In that regard, one of the most challenging issues for AI is the implementation of neural network components in hardware. [2–5] The classical biological neural circuit consists of neurons interconnected by synapses that modulate the inter-neuron signal transfer. The main building block of the brain, *i.e.*, the biological neuron, accumulates incoming signals during the "integration time" and "fires" (generates an output signal) once the integration reaches a threshold. The creation of artificial neurons requires therefore materials possessing a physical property able to implement both Integrate and Fire functionalities with a clear identification of the physical quantity that is integrated [3,6,7]. One of the possible solutions, currently under investigation, is the use of a class of quantum materials, the Mott insulators, [8–10] which exhibits an insulator to metal transition (IMT) under electric field, the so-called Electric Mott Transition (EMT) [11]. The main signature of this EMT is a resistive switching occurring under electric field and which has been explained by different mechanisms depending on the investigated Mott materials. For VO_2, the resistive switching was proposed to originate from the self-Joule heating generated during the electric pulse [11,12,13]. Conversely, in the Mott insulators AM_4Q_8, $(V_{1-x}Cr_x)_2O_3$ and $NiS_{2-x}Se_x$, the resistive switching was associated with the creation of hot carriers followed by an electronic avalanche phenomenon [15–17]. As, several recent studies show impact of light on the Mott transition [18–20], we have reinvestigated here the resistive switching mechanism of a $GaTa_4Se_8$ crystal thanks to a pump-pump-probe experiment with simultaneous electric and laser pulse excitation and electrical conductivity probing. Our study shows that photo-doping provided by laser pulse impacts the EMT transition dynamics. By tuning the number of photogenerated carriers and the energy provided to the system, we shed light on the physical

quantity that is integrated in this Mott material [21] and establish the proof-of-concept of an artificial electro-optical "Mott" neuron.

2. EXPERIMENTAL DETAILS

A. Sample preparation and characterization:

$GaTa_4Se_8$ crystals were synthesized by a method described elsewhere [34], and cleaved into 200 - 300 µm pieces. Crystals used for transport measurements were contacted using 10µm gold wires and carbon paste (Electrodag PR-406), and then annealed under vacuum at 150 °C for 30 min. The low-bias resistance was measured using a Keithley 236 source-measure unit by a standard two- or four-probe technique (Figure 1 a). For the application of electric pulses, we have connected two gold wires along the crystal surface on which light should be applied. The inter-electrode distance was around 200 µm.

B. Pump – pump – probe experiments

We have applied two “pumps”, a ≈ 100 µs electric pulse and a 100 fs laser pulse in a single-shot mode, on the $GaTa_4Se_8$ crystal, as we recorded the evolution of the electric resistance (“probe”). We used a Ti: Sapphire femtosecond laser synchronized with an electric pulse generator (Keithley 8114A) so that the laser output was triggered precisely with the first nanoseconds of the electrical pulse. During the pulse, the voltage and current across the sample were measured with a Tektronix DPO3034 oscilloscope associated with IeS-ISSD210 differential probes. We used an optical parametric amplifier (OPA) to tune the laser wavelength from the visible to mid-IR region. In order to control crystal temperature, we have used a nitrogen Cryostream. We carried out the experiments with the same number of absorbed photons by taking care to keep the laser spot size similar at the different wavelengths. We used a short focus (5 cm) optical lens. After the experiment on the $GaTa_4Se_8$ single crystal, we have performed knife-edge measurements to recover the spatial profile of the laser beam. It allows a reliable estimate of the beam size, which were similar for both laser energies (0.5 and 2.3 eV) and covered more than 90 % of the inter-electrode area. In these experiments, the level of

photodoping depends on both the laser fluence and the impacted volume. The latter is defined by the size of the beam hitting the sample surface and a characteristic length over which the photocarrier spread inside the materials. Since photodoped carriers are subjected to applied DC electric fields E close to 3 kV / cm, this characteristic length corresponds to the diffusion length of the carriers rather than the initial absorption length (*i.e.*, the light penetration depth). The diffusion length is indeed defined as $l_{diff} = \mu.E.\tau$, where μ and τ are the carriers mobility and lifetime, respectively. Considering a lifetime of 1 µs typical of AM_4Q_8 compounds [35] and a mobility representative of Mott insulators of 1 $cm^2.V^{-1}.s^{-1}$ [36] leads to a lower limit of 30 µm for the diffusion length. This value exceeds the typical light penetration depth by more than two orders of magnitude. Consequently, experiments conducted with similar beam sizes and density of absorbed photons, but with laser pulses at different wavelengths, will yield analogous levels of photodoping.

3. RESULTS AND DISCUSSION

According to conventional band theory, Mott insulators should be metallic. Their insulating ground state results from the on-site electron-electron Coulombian repulsion, not accounted for in the classical approach, which favors the localization of electrons on atomic sites. At equilibrium, the insulating state can be broken by pressure or charge doping. Recently, an Insulator to Metal transition leading to a resistive switching was also achieved under electric field in Mott insulators [22,23,15,11]. This phenomenon, also called Electric Mott Transition (EMT), was observed for numerous examples of Mott insulators. In this paper, we focus on a member of the family of narrow gap chalcogenide Mott insulators of formulation AM_4Q_8 (A=Ga, Ge; M = V, Nb, Ta, Mo; Q= S, Se) that exhibit a clustered lacunar spinel structure [24–27]. **Figure 1** presents the thermal dependence of the resistivity and a typical resistive switching phenomenon observed in a crystal of $GaTa_4Se_8$. For this compound, the proposed microscopic mechanism for resistive switching is based on Fröhlich's theory of dielectric breakdown [28,29].

The details of this theory and its application to the AM_4Q_8 Mott insulators were published elsewhere [16]. The model considers the existence of small numbers of electrons either trapped in localized levels below the conduction band or delocalized in the conduction band. These last pre-existing free carriers can be accelerated under electric field and share their energy with other electrons and the lattice thanks to, respectively, electron-electron (e-e) or electron-phonon (e-ph) interactions [16]. New hot carriers are generated under electric field, which increases the overall electronic temperature until a new equilibrium situation is reached between the power given to (electric power) and the power taken out from (e-ph) the electronic system (i.e. it corresponds to a two temperatures model with the electronic temperature stabilizing slightly over that of the lattice) . But once the applied electric field reaches a threshold value E_{th}, the equilibrium between the lattice and electronic sub-systems cannot be maintained, and the system enters into a nonequilibrium state with the number of hot carriers diverging and inducing an IMT (*i.e.* the resistive switching). The theory predicts a temperature-independent deviation from Ohm's law below the threshold field ($E \ll E_{th}$) with the multiplication rate of new carriers in the conduction band $\tilde{n} = {}^{n}/_{n_0}$ depending only on the square of the electric field if we assume the mobility to be constant :

$$\tilde{n} = \frac{n}{n_0} = \frac{\sigma(E)}{\sigma_0} = exp\left(\frac{E^2 \varepsilon_G}{E_{th}^2 e \Delta\varepsilon}\right) \quad (1)$$

where n_0 and σ_0 are the number of carriers and conductivity at zero field. Constants ε_G, $\Delta\varepsilon$ represent the width of the gap and of the in gap state levels, respectively, and e is Euler's constant. In the boundary case of the prediction ($E = E_{th}$), the threshold value of the carrier multiplication rate $\tilde{n}_{th}$ becomes :

$$\tilde{n}_{th} = exp\left(\frac{\varepsilon_G}{\Delta\varepsilon}\right) \quad (2)$$

In our previous work, the low field conductivity of the narrow gap Mott insulators AM_4Q_8 was compared to these predictions using the experimental values for the gap ε_G and for $\Delta\varepsilon$ (*e.g.* ε_G

= 158 meV and $\Delta\varepsilon$ = 112 meV in the case of $GaTa_4Se_8$) [16]. As displayed in **Figure 2**a, the measurements, performed at different temperatures for a $GaTa_4Se_8$ crystal, lie on the predictable master curve for the carrier multiplication rate $\tilde{n}$ (see blue line). It fully supports the proposed model suggesting that, below the threshold field, $\tilde{n}$ may stabilize in time, while above the threshold electric field (≡ when the system exceeds the threshold carrier multiplication rate $\tilde{n}_{th}$ slightly greater than 4 in our experiments) $\tilde{n}$ can not stabilize anymore and may diverge in time. Figure 2 b presents the experimental conductivity ratio dynamics $\tilde{\sigma} = \sigma/\sigma_0$ measured under electric field for a $GaTa_4Se_8$ crystal. Below E_{th} (ranging from 0.3 to 7 kV/cm in $GaTa_4Se_8$ depending on the temperature [16]), the conductivity ratio stabilizes over time and the system remains insulating, which means the electronic temperature reaches an equilibrium. But for electric field higher than the threshold value ($E > E_{th}$) a sudden increase of the conductivity ratio appears (*i.e.* a volatile resistive switching occurs) as the carrier multiplication rate approaches $\tilde{n}_{th}$ and the system enters into an avalanche carrier multiplication regime (Figure 2 a).

According to the model, new hot carriers are accumulated in the AM_4Q_8 compounds under electric field. This model is therefore of great interest in the framework of neurocomputing as it suggests that the AM_4Q_8 compounds behave as hot carrier integrators. Similar to biological neurons that accumulate charges on their membranes until the membrane potential reaches a threshold, the Mott insulators would accumulate hot carriers until the carrier multiplication rate reaches a threshold. In order to support this scenario, we have compared the carrier multiplication rate dynamics obtained under electric pulse alone or when the electric pulse is coupled to a laser pulse in order to modify the carriers number. The setup sketched in **Figure 3** was used to implement this electro-optical pump -and electric probe experiment. A freshly cleaved surface of a $GaTa_4Se_8$ single crystal was connected by two gold electrodes separated by about 200 µm to allow the use of ultrashort laser pulses with a fixed spot size slightly smaller than the inter-electrodes distance. We used a femtosecond Ti:Sapphire regenerative amplifier and an Optical Parametric Amplifier (OPA) to

tune the wavelength of the optical pump between visible and infrared. The electrodes are used both to apply the electric field thanks to a pulse generator and to monitor conductivity dynamics thanks to an oscilloscope connected in parallel. The setup worked in single-shot mode with a synchronous application of the electric and laser pulses. We performed all experiments under nitrogen cryostream cooling at 85(±5) K in order to have optimal stability conditions to induce the resistive switching experiments.

In a first series of experiments, we simultaneously applied electrical voltage pulses of 60V (*i.e.* exceeding the threshold value) and 800 nm ($h\nu$ = 1.55 eV) femtosecond pulses, while varying the excitation density. As depicted in Figure 3a, the main idea was to tune the number of photoexcited carriers at the beginning of the electric pulse. Figure 3a shows that the concomitant application of an optical excitation drastically reduces the time delay necessary to observe the resistive switching. Moreover, this time delay decreases when the excitation density increases. These experiments already evidence a clear impact of photoexcited carriers on the resistive switching. They suggest a similar role of hot carriers generated by light or electric field. This result supports that the photoexcited carriers are added to the hot electrons accumulated under electric field to reach the threshold carrier multiplication rate and promote the avalanche phenomenon. A possible impact of the thermal energy injected into the system (lattice and electrons) by the light pulse cannot be completely discarded based on this experiment alone as at the probed time scale both sub-systems should have reached thermal distributions (Fermi-Dirac and Bose-Einstein).

Another way to address this issue is to tune the excitation density and the photon energy of the pulse using the OPA. As sketched in Figure 3b, the main objective of these experiments is to tune the photon energy while keeping a constant number of photons. This series of experiments were conducted using another $GaTa_4Se_8$ crystal in a configuration similar to that depicted in Figure 3a. The boundary values of the photon energies used ($h\nu$) were 0.5 eV and 2.3 eV. The fluence was set to 2.5 µJ/pulse for $h\nu$ = 0.5 eV and to 8.8 uJ/pulse for $h\nu$ = 2.3 eV. These values

correspond to 7.10^{16} and $5{,}5.10^{16}$ absorbed photons per cm^2, respectively, and hence to almost similar densities of photodoped carriers (see discussion in the experimental section). Electrical measurements presented in Figure 3b demonstrate no change in carrier multiplication rate dynamics under electric field independently of the used photon energies (0.5 eV and 2.3 eV, respectively). In particular, the time delays required to reach $\tilde{n}_{th}$ (*i.e.* the resistive switching) are remarkably similar while the energy provided by the light pulses changes by a factor ≈ 3.5 (8.8 µJ against 2.5 µJ). It demonstrates that the key parameter of the optical excitation that controls the resistive switching *is not* a trivial photothermal effect in agreement with a recent study on the V_2O_3 antiferromagnetic Mott insulating phase [30]. Conversely, it suggests that the relevant parameter driving the Electric Mott Transition in $GaTa_4Se_8$ is rather the number of hot carriers generated. Mott insulators appear therefore as hot carriers integrators that undergo a resistive switching when the carrier multiplication rate ($\tilde{n}$) reaches a threshold value depending only on intrinsic material features/properties.

All these findings are of great interest to build up an electro-optical Mott neuron for artificial neuromorphic devices [3,5] and neuromorphic photonics [31,32]. As depicted in **Figure 4** a, when a biological neuron receives input spikes from other neurons, they are integrated into the membrane potential. In between the incoming spikes, the membrane potential relaxes, which is known as a leaky behavior. Finally, when the membrane potential reaches a threshold value, the neuron triggers an output action potential (Firing event). The biological neuron implements, therefore, three important functionalities that are at the basis of the most used model of an artificial neuron, namely the Leaky, Integrate and Fire (LIF) artificial neuron. In a previous work, we have demonstrated that the AM_4Q_8 compounds, as well as other Mott insulators, like $(V_{1-x}Cr_x)_2O_3$ or [Au(iPr-thiazdt)2] behave as LIF artificial neurons [9]. This behavior was observed when a crystal of Mott insulator was subjected to a train of electrical pulses. **Figure 5**(a-c) shows the results of other experiments intended to control the Mott neuron also by light, and for which an ultrashort laser pulse was synchronized with the first electrical pulse of the

train. These experiments were conducted by applying the train of electrical pulses and laser pulses on a $GaTa_4Se_8$ crystal using a similar setup as shown in Figure 4b. The green curves in Figure 5b, represent conductivity ratio or carrier multiplication rate measured without laser. When electric pulses of 63V are applied, the system fires (*i.e.* a resistive switching is observed) during the fifth pulse while no firing event is observed when pulses of 52V are used. Applying a laser pulse (10μJ/pulse, $h\nu$ = 1.55 eV) at the beginning of the train of electric pulses has a strong impact on the behavior of the Mott neuron. Indeed, the firing event occurs much sooner compared to the case without optical excitation. For electrical pulses of 63V, it occurs after only two electrical pulses while it appears in the fifth pulse when using 52 V (see violet curves). There is a striking difference as no firing event is recorded with electrical stimulus only. These experiments demonstrate a clear impact of an ultrashort light pulse on the behavior of the Mott artificial neuron. It reveals that ultrashort light pulses could be used as a new external parameter to tune the Firing time of the device. At this step the device is made with a single crystal and for this reason the LIF behavior is observed at low temperature using quite high voltage pulses. But our previous works on Mott artificial Mott neuron have already demonstrated that the working conditions can be much improved by using thin film devices [9,33]. Indeed the downscaling of thin film device allows to lower the operational voltage to a few volts and to increase the working temperatute towards room temperature. The experiments reported in this paper and performed on single crystals open, therefore, the door to the realization of artificial electro-optical Mott neurons made of thin films that would be promising components for neuromorphic photonics These experiments open, therefore, the door to the realization of artificial electro-optical Mott neurons which are promising components for neuromorphic photonics [31,32].

4. CONCLUSIONS

To conclude, the electro-optical pump -electrical probe measurements presented in this work

demonstrate the possibility to control the dynamics of the Electric Mott transition by ultrashort laser pulses in the Mott insulator $GaTa_4Se_8$. It further confirms that light and electric field can act synergistically to induce an insulator to metal transition in a Mott insulator. These results are compatible with an Electric Mott transition mechanism based on a carrier multiplication phenomenon whose dynamics can be modified thanks to the generation of extra photo-carriers by optical excitation. The obtained results demonstrate that Mott insulators behave under electric field as leaky integrators of hot carriers, more precisely of carrier multiplication rate. When the carrier multiplication rate reaches a threshold value, the firing event (i.e., the resistive switching) occurs. Hot carriers and carrier multiplication rates are, therefore, the physical quantities of interest to control the Mott Neuron. Beyond this fundamental output, we have also shown that both light and electric field stimuli can control the dynamics of the Mott artificial neuron. Our work demonstrates an interesting concept of electro-optical artificial Mott neuron and opens an alternative path in the emerging field of neuromorphic photonics [31,32].

ACKNOWLEDGEMENTS

All authors gratefully acknowledge Agence Nationale de la Recherche for financial support under grant ANR-16-CE30-0018 (“Elastica”). DB thanks University of Nantes for financial support in the framework of the IM-LED LIA (CNRS).

References

[1] A. K. Jain, J. Mao, and K. M. Mohiuddin, *Artificial Neural Networks: A Tutorial*, Computer **29**, 31 (1996).
[2] J. Misra and I. Saha, *Artificial Neural Networks in Hardware: A Survey of Two Decades of Progress*, Neurocomputing **74**, 239 (2010).
[3] G. Indiveri and T. K. Horiuchi, *Frontiers in Neuromorphic Engineering*, Front Neurosci **5**, (2011).
[4] D. Seok Jeong, I. Kim, M. Ziegler, and H. Kohlstedt, *Towards Artificial Neurons and Synapses: A Materials Point of View*, RSC Advances **3**, 3169 (2013).
[5] J. Zhu, T. Zhang, Y. Yang, and R. Huang, *A Comprehensive Review on Emerging Artificial Neuromorphic Devices*, Applied Physics Reviews **7**, 011312 (2020).
[6] A. N. Burkitt, *A Review of the Integrate-and-Fire Neuron Model: I. Homogeneous Synaptic Input*, Biol Cybern **95**, 1 (2006).
[7] *A Review of the Integrate-and-Fire Neuron Model: I. Homogeneous Synaptic Input. - ResearchGate*, (2006).
[8] P. Stoliar, J. Tranchant, B. Corraze, E. Janod, M.-P. Besland, F. Tesler, M. Rozenberg, and L. Cario, *A Leaky-Integrate-and-Fire Neuron Analog Realized with a Mott Insulator*, Advanced Functional Materials **27**, 1604740 (2017).
[9] C. Adda, B. Corraze, P. Stoliar, P. Diener, J. Tranchant, A. Filatre-Furcate, M. Fourmigué, D. Lorcy, M.-P. Besland, E. Janod, and L. Cario, *Mott Insulators: A Large Class of Materials for Leaky Integrate and Fire (LIF) Artificial Neuron*, Journal of Applied Physics **124**, 152124 (2018).
[10] F. Tesler, C. Adda, J. Tranchant, B. Corraze, E. Janod, L. Cario, P. Stoliar, and M. Rozenberg, *Relaxation of a Spiking Mott Artificial Neuron*, Phys. Rev. Applied **10**, 054001 (2018).
[11] E. Janod, J. Tranchant, B. Corraze, M. Querré, P. Stoliar, M. Rozenberg, T. Cren, D. Roditchev, V. T. Phuoc, M.-P. Besland, and L. Cario, *Resistive Switching in Mott Insulators and Correlated Systems*, Adv. Funct. Mater. **25**, 6287 (2015).
[12] B. S. Mun, J. Yoon, S.-K. Mo, K. Chen, N. Tamura, C. Dejoie, M. Kunz, Z. Liu, C. Park, K. Moon, and H. Ju, *Role of Joule Heating Effect and Bulk-Surface Phases in Voltage-Driven Metal-Insulator Transition in VO2 Crystal*, Applied Physics Letters (2013).
[13] S. Kumar, M. D. Pickett, J. P. Strachan, G. Gibson, Y. Nishi, and R. S. Williams, *Local Temperature Redistribution and Structural Transition During Joule-Heating-Driven Conductance Switching in VO2*, Adv. Mater. **25**, 6128 (2013).
[14] A. Zimmers, L. Aigouy, M. Mortier, A. Sharoni, S. Wang, K. G. West, J. G. Ramirez, and I. K. Schuller, *Role of Thermal Heating on the Voltage Induced Insulator-Metal Transition in VO_{2}*, Phys. Rev. Lett. **110**, 056601 (2013).

[15] V. Guiot, L. Cario, E. Janod, B. Corraze, V. Ta Phuoc, M. Rozenberg, P. Stoliar, T. Cren, and D. Roditchev, *Avalanche Breakdown in GaTa4Se8−xTex Narrow-Gap Mott Insulators*, Nat Commun **4**, 1722 (2013).
[16] P. Diener, E. Janod, B. Corraze, M. Querré, C. Adda, M. Guilloux-Viry, S. Cordier, A. Camjayi, M. Rozenberg, M. P. Besland, and L. Cario, *How a Dc Electric Field Drives Mott Insulators Out of Equilibrium*, Phys. Rev. Lett. **121**, 016601 (2018).
[17] P. Stoliar, L. Cario, E. Janod, B. Corraze, C. Guillot-Deudon, S. Salmon-Bourmand, V. Guiot, J. Tranchant, and M. Rozenberg, *Universal Electric-Field-Driven Resistive Transition in Narrow-Gap Mott Insulators*, Advanced Materials **25**, 3222 (2013).
[18] E. Abreu, D. Babich, E. Janod, S. Houver, B. Corraze, L. Cario, and S. Johnson, *THz Driven Dynamics in Mott Insulator GaTa $_4$ Se $_8$*, in *2019 44th International Conference on Infrared, Millimeter, and Terahertz Waves (IRMMW-THz)* (IEEE, Paris, France, 2019), pp. 1–2.
[19] H. Yamakawa, T. Miyamoto, T. Morimoto, T. Terashige, H. Yada, N. Kida, M. Suda, H. M. Yamamoto, R. Kato, K. Miyagawa, K. Kanoda, and H. Okamoto, *Mott Transition by an Impulsive Dielectric Breakdown*, Nature Mater **16**, 1100 (2017).
[20] F. Giorgianni, J. Sakai, and S. Lupi, *Overcoming the Thermal Regime for the Electric-Field Driven Mott Transition in Vanadium Sesquioxide*, Nature Communications **10**, 1 (2019).
[21] J. Tranchant, E. Janod, B. Corraze, P. Stoliar, M. Rozenberg, M.-P. Besland, and L. Cario, *Control of Resistive Switching in AM4Q8 Narrow Gap Mott Insulators: A First Step towards Neuromorphic Applications*, Phys. Status Solidi A **212**, 239 (2015).
[22] Y. Taguchi, T. Matsumoto, and Y. Tokura, *Dielectric Breakdown of One-Dimensional Mott Insulators Sr 2 CuO 3 and SrCuO 2*, Physical Review B **62**, 7015 (2000).
[23] G. Stefanovich, A. Pergament, and D. Stefanovich, *Electrical Switching and Mott Transition in VO2*, Journal of Physics: Condensed Matter **12**, 8837 (2000).
[24] H. B. Yaich, J. C. Jegaden, M. Potel, R. Chevrel, M. Sergent, A. Berton, J. Chaussy, A. K. Rastogi, and R. Tournier, *Nouveaux Chalcogenures Mixtes GaMo4(XX')8 (X =S, Se, Te) à Clusters Tetraedriques Mo4*, Journal of Solid State Chemistry **51**, 212 (1984).
[25] R. Pocha, D. Johrendt, B. Ni, and M. M. Abd-Elmeguid, *Crystal Structures, Electronic Properties, and Pressure-Induced Superconductivity of the Tetrahedral Cluster Compounds GaNb $_4$ S $_8$, GaNb $_4$ Se $_8$, and GaTa $_4$ Se $_8$*, Journal of the American Chemical Society **127**, 8732 (2005).
[26] D. Bichler, V. Zinth, D. Johrendt, O. Heyer, M. K. Forthaus, T. Lorenz, and M. M. Abd-Elmeguid, *Structural and Magnetic Phase Transitions of the V4-Cluster Compound GeV4S8*, Phys. Rev. B **77**, 212102 (2008).
[27] V. Guiot, E. Janod, B. Corraze, and L. Cario, *Control of the Electronic Properties and Resistive Switching in the New Series of Mott Insulators GaTa4Se8–YTey (0 ≤ y ≤ 6.5)*, Chem. Mater. **23**, 2611 (2011).
[28] H. Fröhlich and N. F. Mott, *Theory of Electrical Breakdown in Ionic Crystals*, Proceedings of the Royal Society of London. Series A - Mathematical and Physical Sciences **160**, 230 (1937).
[29] H. Fröhlich and N. F. Mott, *On the Theory of Dielectric Breakdown in Solids*, Proceedings of the Royal Society of London. Series A. Mathematical and Physical Sciences **188**, 521 (1947).
[30] A. Ronchi, P. Franceschini, P. Homm, M. Gandolfi, G. Ferrini, S. Pagliara, F. Banfi, M. Menghini, J.P. Locquet, and C. Giannetti, *Light-Assisted Resistance Collapse in a V 2 O 3 -Based Mott-Insulator Device*, Phys. Rev. Applied **15**, 044023 (2021).
[31] E. Goi, Q. Zhang, X. Chen, H. Luan, and M. Gu, *Perspective on Photonic Memristive Neuromorphic Computing*, PhotoniX **1**, 3 (2020).
[32] P. R. Prucnal and B. J. Shastri, *Neuromorphic Photonics* (CRC Press, 2017).

[33] C. Adda, L. Cario, J. Tranchant, E. Janod, M.-P. Besland, M. Rozenberg, P. Stoliar, and B. Corraze, *First Demonstration of "Leaky Integrate and Fire" Artificial Neuron Behavior on (V0.95Cr0.05)2O3 Thin Film*, MRS Communications **8**, 835 (2018).
[34] C. Vaju, L. Cario, B. Corraze, E. Janod, V. Dubost, T. Cren, D. Roditchev, D. Braithwaite, and O. Chauvet, *Electric-Pulse-Driven Electronic Phase Separation, Insulator–Metal Transition, and Possible Superconductivity in a Mott Insulator*, Advanced Materials **20**, 2760 (2008).
[35] D. Babich, K. Fukumoto, B. Corraze, J. Tranchant, M. Lorenc, H. Cailleau, S.-Y. Koshihara, L. Cario, and E. Janod, *Unusually Long Carrier Lifetime in a Mott Insulator Revealed by Time-Resolved Photoemission Electron Microscopy*, in *Frontiers in Optics + Laser Science APS/DLS (2020), Paper LTu8F.3* (Optical Society of America, 2020), p. LTu8F.3.
[36] J. C. Petersen, A. Farahani, D. G. Sahota, R. Liang, and J. S. Dodge, *Transient Terahertz Photoconductivity of Insulating Cuprates*, Phys. Rev. B **96**, 115133 (2017).

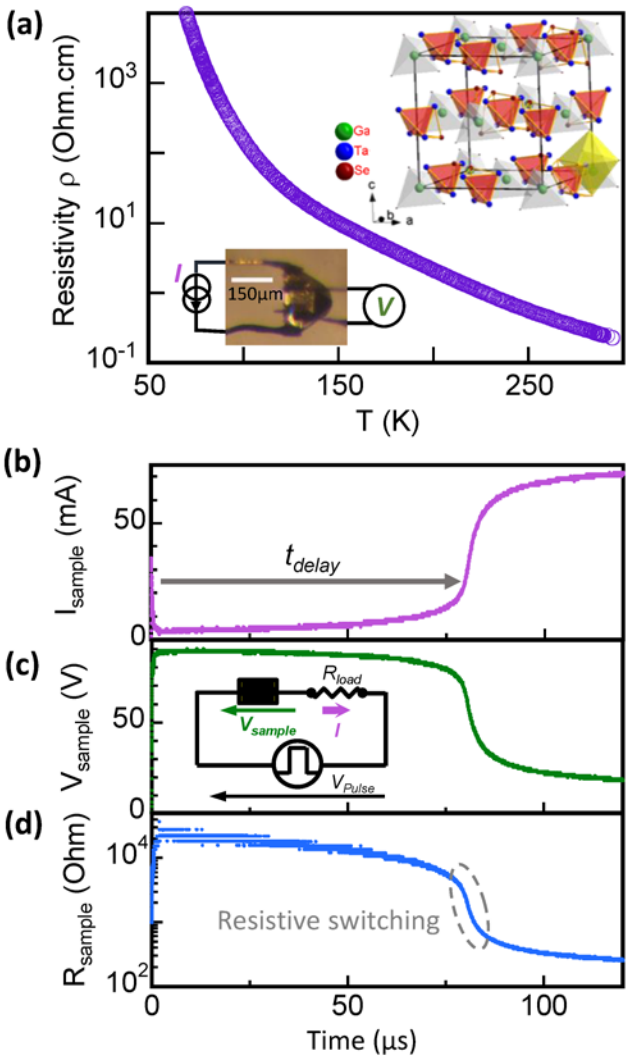

Figure 1 **:** (a) Resistivity versus temperature measured on a single crystal of the Mott insulator $GaTa_4Se_8$. The inset shows the crystallographic structure of $GaTa_4Se_8$ and a picture of the $GaTa_4Se_8$ single crystal connected with four gold wires. (b-d) A typical example of an Electric Mott Transition induced at 85 K by the application of a 120 µs / 90 V electric pulse on a circuit made of the $GaTa_4Se_8$ crystal in series with a 1 kΩ load resistance. The temporal evolutions of the current (b), of the sample voltage (c), and of the sample resistance (d) clearly indicate a resistive switching occurring after a time delay of ≈ 80 µs.

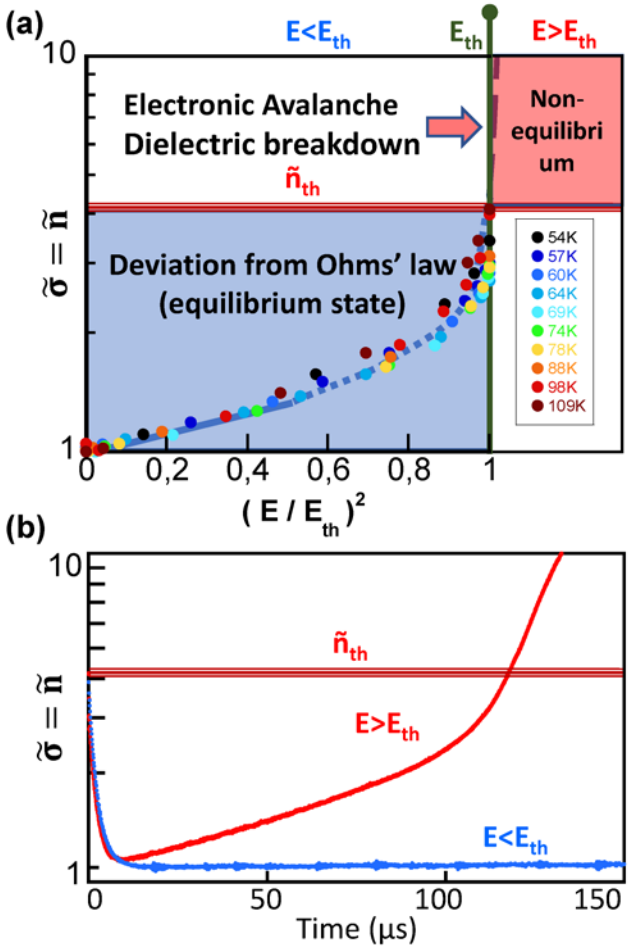

Figure 2 : (a) Transport measurements performed at different temperatures and low electric field for a $GaTa_4Se_8$ crystal. All measurements fall on a master curve following the predicted evolution of the carrier multiplication rate $\tilde{n}$ (Blue dotted line). (b) Conductivity ratio dynamics $\tilde{\sigma} = \sigma/\sigma_0$ measured under electric field for a $GaTa_4Se_8$ crystal for $E < E_{th}$ and $E > E_{th}$.

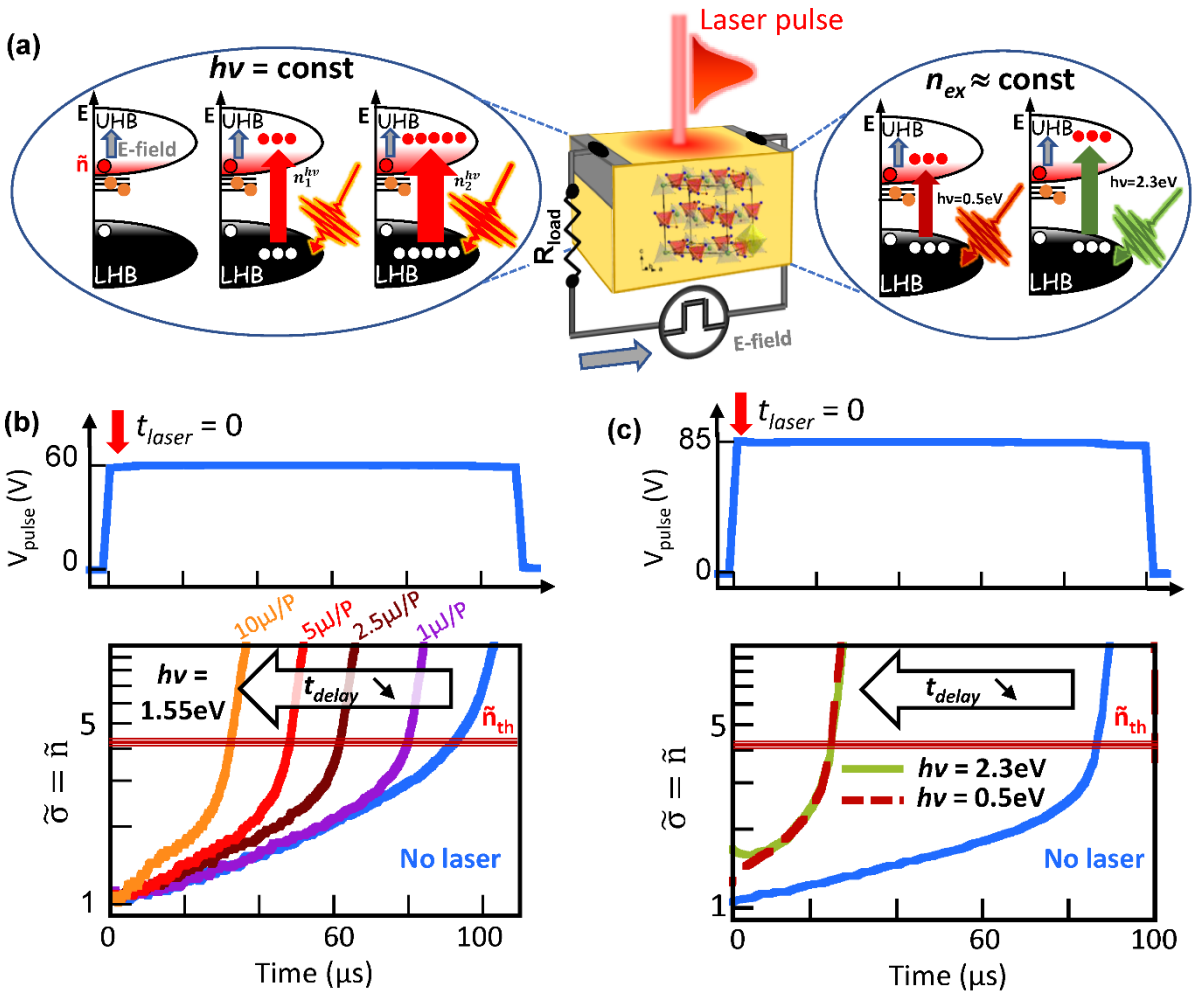

Figure 3 **:** Temporal evolution of the normalized conductivity $\tilde{\sigma} = \sigma / \sigma_0$ during a voltage pulse applied to different circuits containing a $GaTa_4Se_8$ crystal and which is synchronized or not with a single-shot 100 fs laser pulse applied at the beginning of the pulse. (a) Schematic representation of the setup and impact of laser fluence or wavelength on the number of electrons excited from the Lower (LHB) to the Upper Hubbard Band (UHB). (b) Evolution of $\tilde{\sigma}(t)$ measured under a 60V voltage pulse and when fs laser pulses of constant energy (800 nm, $h\nu$ = 1.55 eV) and of increasing fluences are applied (from 1µJ/Pulse to 10 µJ/P). (c) Evolution of $\tilde{\sigma}(t)$ measured on a different $GaTa_4Se_8$ crystal under a 85 V voltage pulse and when fs laser pulses leading to the same number of induced photocarriers are applied with two different energies ($h\nu$ = 0.5 and 2.3 eV).

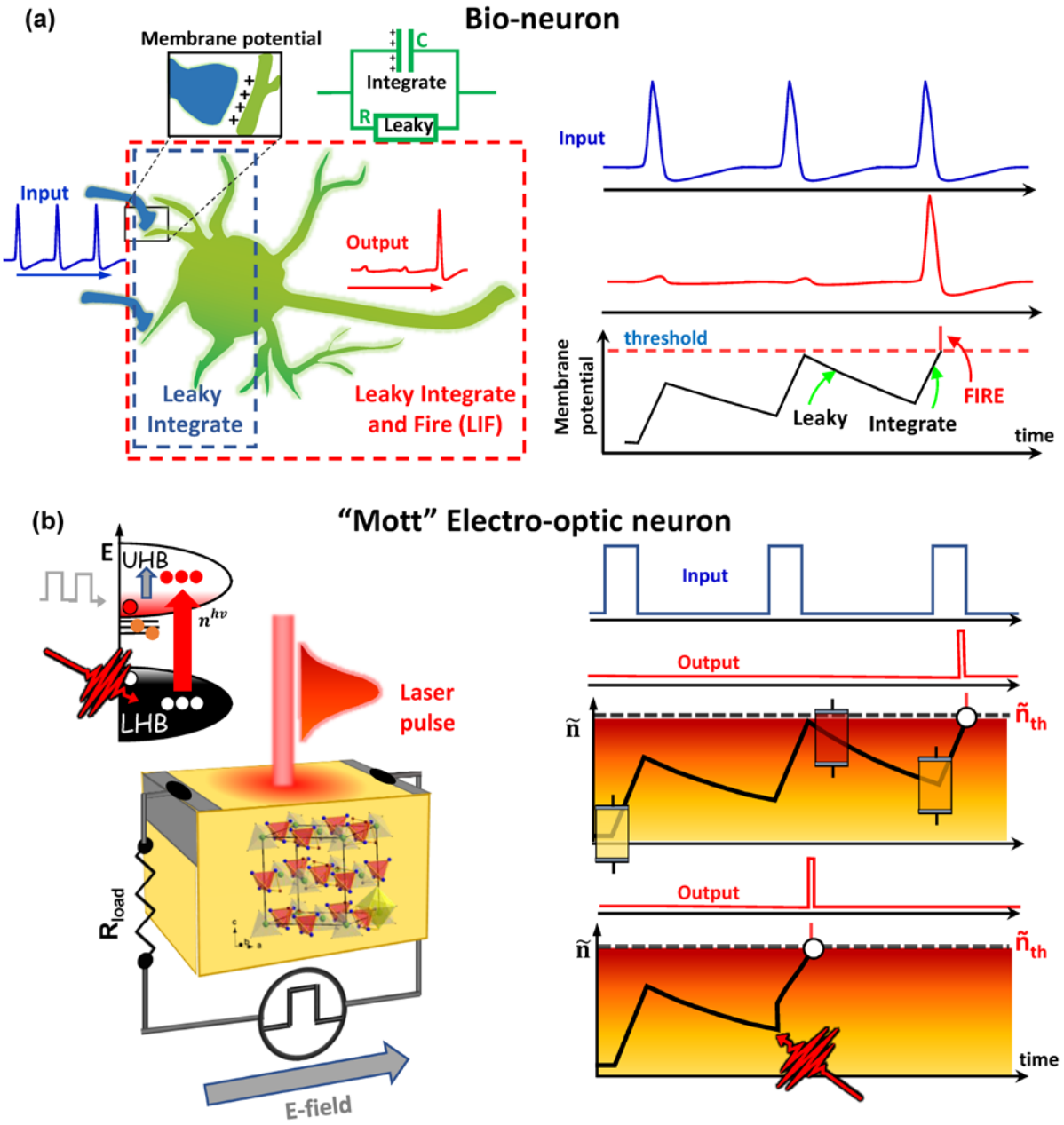

Figure 4 : (a) Schematic picture of a biological neuron receiving input spikes from other neurons and triggering an output action potential when the membrane potential reaches a threshold value. This behavior of the neuron membrane was first modeled by a RC circuit and led to the definition of the simplest model of artificial neuron called "Leaky integrate and Fire (LIF)" (b) Sketch of an electro-optic Mott neuron setup and graphical representation of the electronic dynamics with or without laser pulse. The artificial Mott neuron follows a similar dynamics as the LIF model but the integrated quantity is not the membrane potential (or the charge in the capacitor) but the carriers multiplication rate (ñ) in the Mott device.

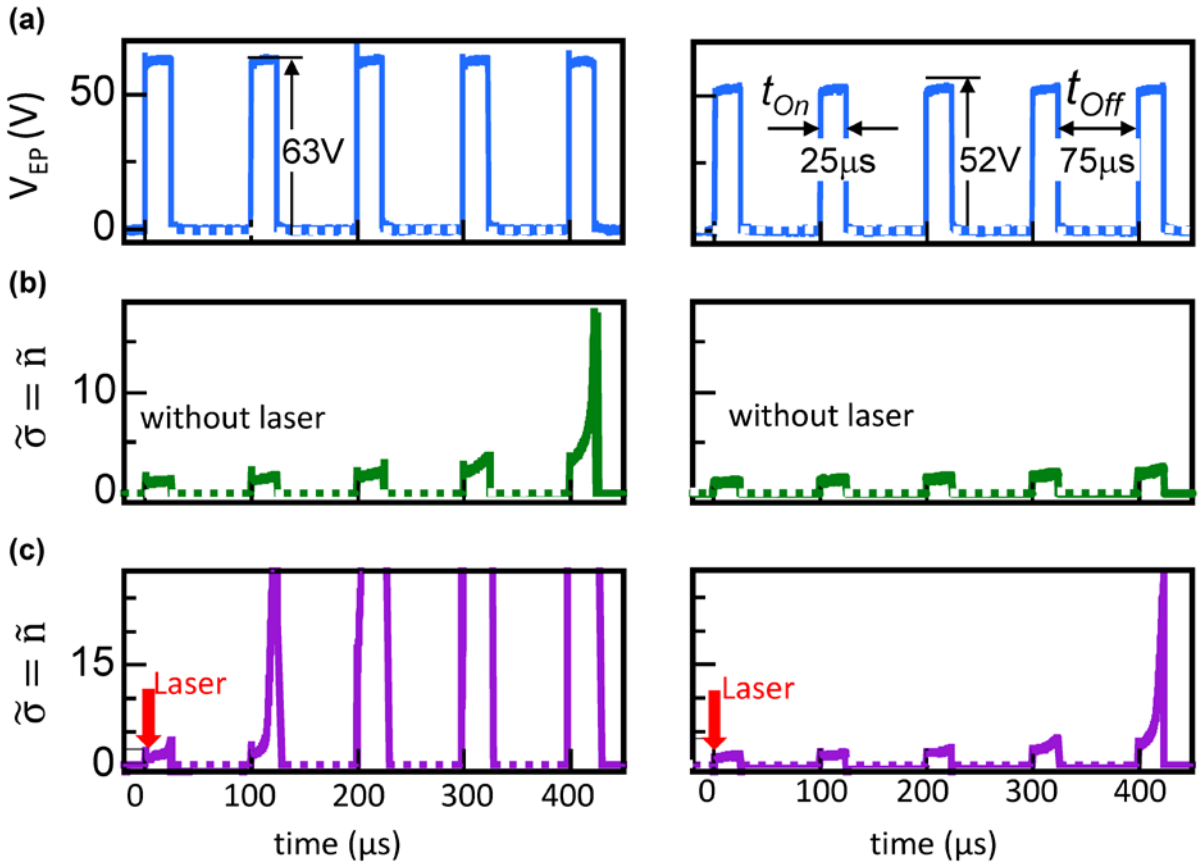

Figure 5 : Experimental resistive switching obtained by applying trains of 25µs electric pulses of 63 V or 52 V synchronized or not with a 100 fs laser pulse. (a) Profile of applied voltage pulses, b) and c) sample conductivity time profiles measured without and with laser pulse, respectively. The measurements were performed in similar conditions to the ones of Figure 3 a.